Environmental Science & Technology

pubs.acs.org/est

Article

Global Decarbonization Enabled by a Novel Strategy of Biomineralization for Concrete Corrosion Inhibition

Xiaohao Sun, Yong Wang, Jiadong Ren, Onyx W.H. Wai, and Xiangdong Li*

Cite This: *Environ. Sci. Technol.* 2025, 59, 17628−17639

Read Online

ACCESS | Metrics & More | Article Recommendations | Supporting Information

ABSTRACT: With rapid urban population growth, predominantly in coastal regions, decarbonizing concrete structures in coastal cities is crucial. Extending the lifespan of concrete is highly efficient in achieving net-zero greenhouse gas (GHG) emissions by 2050. Biomineralization for concrete corrosion inhibition (BCCI) was previously proposed and demonstrated to effectively protect marine concrete in laboratory experiments, showing promise for decarbonization due to potentially increased lifespans. The potential of BCCI for decarbonization and sustainability warrants further investigation. Therefore, this study evaluated its impact on GHG emissions for insights into global decarbonization. Field corrosion experiments were conducted to ascertain its effectiveness as a valuable GHG calculation input, including biofilm community analysis and microstructure and macroscopic measurements of concrete. Results show that BCCI decreased the total/relative abundances of corrosive bacteria, inhibited sulfate and chloride diffusion, and enhanced carbon functions, irrespective of concrete type. Moreover, BCCI significantly reduced GHG emissions, particularly in 20 MPa concrete. BCCI demonstrated substantial GHG mitigation potential in China, Indonesia, and the USA, which enabled a competitive 37−65% reduction in global GHG from producing underwater concrete. In the long term, this strategy would yield more sustainable development benefits. Findings contribute to achieving global decarbonization and multiple sustainable development goals for concrete sectors and coastal infrastructures.

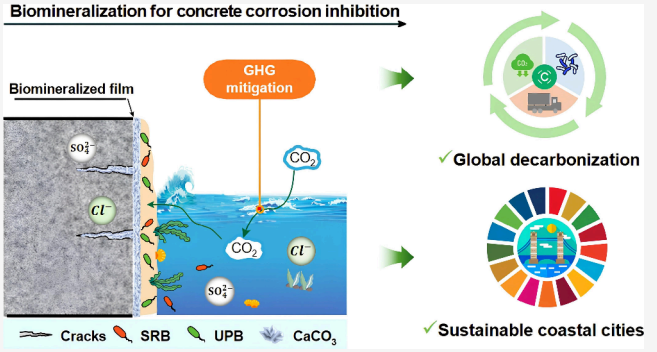

KEYWORDS: *decarbonization, sustainable concrete structures, biomineralization, microbially induced corrosion, GHG emissions*

1. INTRODUCTION

Growing urban populations and deteriorating infrastructure are driving an unprecedented demand for concrete production, which accounts for over 8% of anthropogenic greenhouse gas (GHG) emissions,[1] with material consumption contributing to nearly 50% of GHG emissions.[2,3] To achieve net-zero GHG emissions by 2050, the "difficult-to-decarbonize" industries, such as the concrete sector, must develop effective mitigation strategies.[4] Moreover, urban population growth, predominantly in coastal regions, is projected to outstrip overall population growth,[5] increasing the use of concrete for coastal/marine developments. However, insufficient attention has been paid to the GHG emissions from concrete production in coastal cities and the corresponding decarbonization efforts. Consequently, achieving decarbonization associated with concrete structures in coastal cities holds significant implications on a global scale.

Extending the service life of concrete structures is a highly efficient strategy for mitigating GHG emissions[6] by curtailing the production of new materials.[7] In marine environments, in addition to chemical corrosion from high concentrations of aggressive ions (*e.g.*, sulfate and chloride),[8] microbially induced corrosion (MIC) is also a common phenomenon threatening marine concrete structures worldwide.[9] Compared with chemical corrosion, corrosive bacteria in MIC accelerate concrete degradation,[10] easily causing cracks, significantly reducing the lifespan of concrete structures.[11] The reduced lifespan would lead to increased repair and maintenance requirements, generating additional GHG emissions, and leading to considerable economic losses. Therefore, inhibiting MIC is crucial for sustainable marine concrete structures. However, currently developed methods still have many limitations for inhibiting concrete corrosion.[10,12−16] Therefore, a novel "green" and effective alternative, biomineralization for concrete corrosion inhibition (BCCI), was previously proposed for marine concrete protection, showing superior corrosion inhibition effects on seawater sea-sand concrete

Received: January 18, 2025
Revised: July 12, 2025
Accepted: July 14, 2025
Published: August 14, 2025

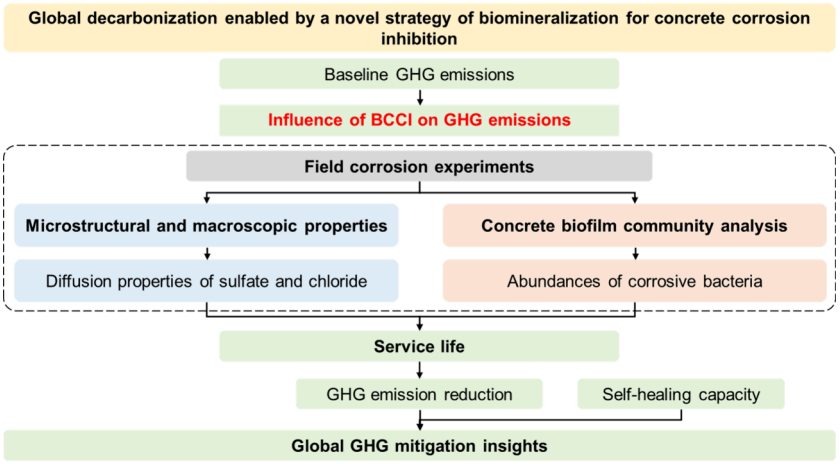

Figure 1. Overall structure of the study. Note: GHG refers to greenhouse gas and BCCI is biomineralization for concrete corrosion inhibition.

(SSC) via laboratory experiments.[17] The BCCI method holds promise for enhancing the durability of concrete structures, beneficial for reducing the frequency of repairs, thereby decreasing the carbon footprint and energy consumption of marine infrastructure during its operational phase, contributing to carbon neutrality and sustainability.[17] The GHG reduction potential of this BCCI strategy warrants further investigation to offer insights into global decarbonization efforts.

In marine environments, corrosive bacteria in MIC can accelerate sulfate corrosion on concrete. Environmental chlorides are typically the most aggressive and detrimental factor behind steel corrosion in marine reinforced concrete structures.[18] The transport of corrosive bacteria in pores or cracks altered ion concentrations in concrete,[19] affecting corrosion depths and diffusion coefficients. The BCCI treatment has been demonstrated to effectively inhibit the diffusion of sulfate and chloride[20] and decrease the abundance of corrosive bacteria. However, the influence of corrosion inhibition on the service life of concrete has not been thoroughly investigated. Therefore, relationships were established between service life and diffusion properties, as well as corrosive bacteria, which were then used to determine the GHG reduction resulting from the BCCI treatment (Figure 1). Furthermore, restricting the application of BCCI to marine concrete alone may result in an underestimation of global decarbonization efforts. To systematically quantify the impact of BCCI on global GHG emissions, the application was extended to underwater concrete structures (*e.g.,* sewage systems, wastewater treatment plants, and marine infrastructure), where concrete corrosion is easily induced by corrosive bacteria[17,21−24] (Section S1, Figure S1). Notably, intricate field environments may impact the treatment efficacies of BCCI compared to previous laboratory studies, potentially influencing the accuracy of GHG calculations. Therefore, a field corrosion experiment was conducted to ascertain the treatment effects of BCCI in real marine environments and to provide valuable inputs to facilitate accurate GHG calculations. Concrete biofilm communities and microstructure and macroscopic properties of concrete specimens were investigated to assess corrosion resistance performances in field environments (Figure S2). According to UN projections, the number of individuals migrating to urban areas will reach 2.3 billion in 2050, leading to accelerated urbanization, necessitating the development of a substantial amount of housing and infrastructure, particularly in coastal cities.[25] This suggests that there will be a wide range of markets for applications of the BCCI strategy in the future. Therefore, the findings will significantly contribute to protecting underwater concrete structures with enhanced corrosion resistance, paving the way for achieving global decarbonization and multiple SDGs.

2. MATERIALS AND METHODS

2.1. Baseline GHG Emissions in Concrete Production. Before evaluating the potential influence on GHG of the proposed BCCI strategy, the baseline GHG emissions in concrete production were first calculated. Specific modeling assumptions were made for individual concrete constituents, transportation, and batching based on the OpenConcrete modeling tool to determine the environmental impacts of cement-based materials.[26] In reference to the previously developed method,[7] an initial cradle-to-gate scope was employed, and comparisons were made on a per cubic meter basis. During the preparation of concrete, we considered and calculated the GHG emissions associated with producing major components and specific processes, taking into account the different compositions of various types of concrete (Table S1). The baseline GHG emissions of concrete were determined corresponding to different compressive strengths (20, 35, and 50 MPa) (details of the methods are presented in Section S2).

2.2. Historical Global GHG Emissions in Underwater Concrete Production. To investigate global GHG emissions in concrete production, data on concrete production were collected from 17 different countries/regions (i.*e.,* UK, USA, New Zealand, France, Colombia, Mainland China, Hong Kong, Taiwan, India, Indonesia, Russia, Turkey, Egypt, Vietnam, Brazil, Saudi Arabia, and Germany). The global averaged GHG emission of concrete (kg CO_2 eq/m^3) was used to conveniently calculate the historical GHG emissions from concrete production across different countries/regions in 2022.[7] Notably, the investigation on decarbonization was extended from marine concrete to underwater concrete because of the application potential of BCCI in different underwater environments. The ratios of underwater concrete to total concrete in different regions (*e.g.,* Asia-Pacific, Middle-East-Africa, Europe, North America, and South America) were first collected according to relevant market research reports[27]

https://doi.org/10.1021/acs.est.5c00261
Environ. Sci. Technol. 2025, 59, 17628−17639

and the GHG emissions from the production of underwater concrete across these 17 different countries/regions were subsequently obtained for comparison. Furthermore, it was imperative to obtain comprehensive global data to underscore the global implications of the BCCI strategy. Therefore, based on the size of the various markets for concrete, data on the underwater concrete production was obtained and the corresponding global GHG emissions were eventually determined (details of the procedures are presented in Section S3).

2.3. Field Corrosion Experiments for Valuable Data Inputs for GHG Calculations. Blended cement concrete (BCC) containing pulverized fuel ash exhibited improved mechanical performance while minimizing the ingress of aggressive ions. SSC, a new type of concrete, also exhibits superior resistance performance compared to ordinary Portland cement concrete (OPCC) when exposed to aggressive ions.[15] However, the efficacy of BCC and new types of concrete in MIC environments remains to be substantiated.[11] Therefore, three different types of concrete (i.e., OPCC, BCC, and SSC) were prepared as representative samples of marine concrete for field corrosion experiments (Section S4, Table S2). All types of concrete specimens were categorized into two groups corresponding to MIC and BCCI, respectively (Table S3). These concrete specimens were put in a field exposure station (Figure S3a) for six months with two exposure zones (i.e., tidal zone and air zone) (Figure S3b) (details of the field corrosion experiment are presented in Section S4).

During the corrosion, the biofilms formed on the concrete surfaces were sampled every three months with high-quality DNA extracted according to the FastDNA Spin Kit for Soil.[28,29] The 16S rRNA gene and β-subunit of the dissimilatory sulfite reductase (*dsrB*) gene were quantified on a StepOnePlus Real-Time PCR System to assess the total bacterial loading and abundance of sulfate-reducing bacteria (SRB), respectively.[30] The metagenomics sequencing of each DNA sample was performed on an MGISEQ-2000 platform[31] with a PE100 strategy. Clean data from the biofilm samples were first obtained[32] and taxonomy classification was conducted[33,34] to compare the bacterial communities at the species level. The α diversity (Shannon index) was calculated and a principal coordinate analysis plot was generated based on the unweighted UniFrac distance metrics.[35] To elucidate the alterations in the sulfur-utilizing bacterial communities during the corrosion, SRB and sulfur-oxidizing bacteria (SOB) profiles in various concrete biofilms were screened out from the total bacterial communities, based on a list of commonly studied SRB and SOB summarized in the literature.[17] In addition, the filtered high-quality reads were assembled to yield contigs ($\geq$1000 bp),[36] which were annotated[37] and subsequently used to predict open reading frames.[38] The open reading frame sequences were assigned putative function predictions[39] to identify Kyoto Encyclopedia of Genes and Genomes orthologs.[40] The functional variability among the substrates with the Kyoto Encyclopedia of Genes and Genomes-based Bray−Curtis dissimilarity was also calculated.[41] Furthermore, sulfur-related and carbon-related functions were isolated to facilitate a comparative analysis of sulfur cycling and carbon cycling[42] (for detailed analysis of bacterial communities and the functional annotations, please refer to Section S5).

The microscopic characteristics of the concrete biofilms were illustrated using scanning electron microscopy (SEM) (TESCAN VEGA3, TESCAN, Czech Republic).[43] X-ray Diffraction (XRD) (Rigaku SmartLab 9 kW-Advance) was used to identify the products of corrosion.[44] In addition, concrete specimens under different conditions were ground into powder at different depth intervals. Sulfate concentrations at different depths were determined using the barium sulfate gravimetric method.[45] Similarly, the chloride levels in concrete were obtained using the traditional silver nitrate titration method.[18] Moreover, the calcium carbonate ($CaCO_3$) content in the formed biomineralized film was measured using the acid pickling method.[46] Compressive strength reduction was also obtained to study corrosion rates (detailed microstructural and macroscopic measurements are presented in Section S6).

2.4. Relationship between Corrosion Inhibition and GHG Emissions. The durability of concrete structures is closely related to the ion diffusion properties of concrete.[7] First, the relationships between service life and the diffusion properties of sulfate and chloride were established (Figure S4). The damage caused by a sulfate attack on concrete can be quantified by considering the diffusion depth of sulfate or the extent of the expansion and the rate of progress because a sulfate attack is commonly described as a reactive transport process.[47] The time to corrosion initiation, defined as corrosion time, was determined based on the diffusion depth to reach steel reinforcement and identified as the service life related to sulfate corrosion. Moreover, the time-depth dependent life prediction model[48] was employed to investigate chloride-related diffusion because actual chloride profiles in concrete at a specific exposure age were obtained in this study through field corrosion experiments. (The details on establishing the relationship between service life and diffusion properties are presented in Section S7).

In addition, a higher abundance of corrosive bacteria also resulted in reduced durability. In this work, a service life prediction model on the concrete in MIC environments was developed based on the total abundance of SRB. The deterioration rate model recommended by the American Concrete Institute[49] was first utilized to calculate corrosion depths in MIC environments. The reliability-based Monte Carlo life prediction method[50] was then used to determine the lifespan of concrete in MIC environments. In this deterioration rate model, the relationship between surface sulfate concentration and the total abundance of SRB was determined in advance by fitting the data in a previous study about MIC on marine concrete.[17] Furthermore, the correlation between the reduction in demand for cement-based materials and the extension of service life was quantified.[7] The influence of reducing the demand for materials on GHG mitigation was then investigated to determine the GHG emissions associated with corrosion inhibition (details on establishing the relationship between service life and corrosive bacteria abundance, as well as GHG emissions, are presented in Sections S8, and S9).

2.5. Influence of the BCCI Strategy on GHG Emissions. The influence of BCCI on the diffusion properties of sulfate and chloride and SRB abundances was investigated in field corrosion experiments, and the obtained data were used to explore the potential mitigation of GHG related to corrosion inhibition, based on the above-established relationships. Notably, in addition to inhibiting corrosion, concrete with BCCI also possesses a self-healing capacity,[51,52] which is beneficial for long-term GHG mitigation similarly due to potentially increased service life.[53] As a result, a comprehensive investigation was conducted to evaluate the combined influences of corrosion inhibition and self-healing on GHG

https://doi.org/10.1021/acs.est.5c00261
Environ. Sci. Technol. 2025, 59, 17628−17639

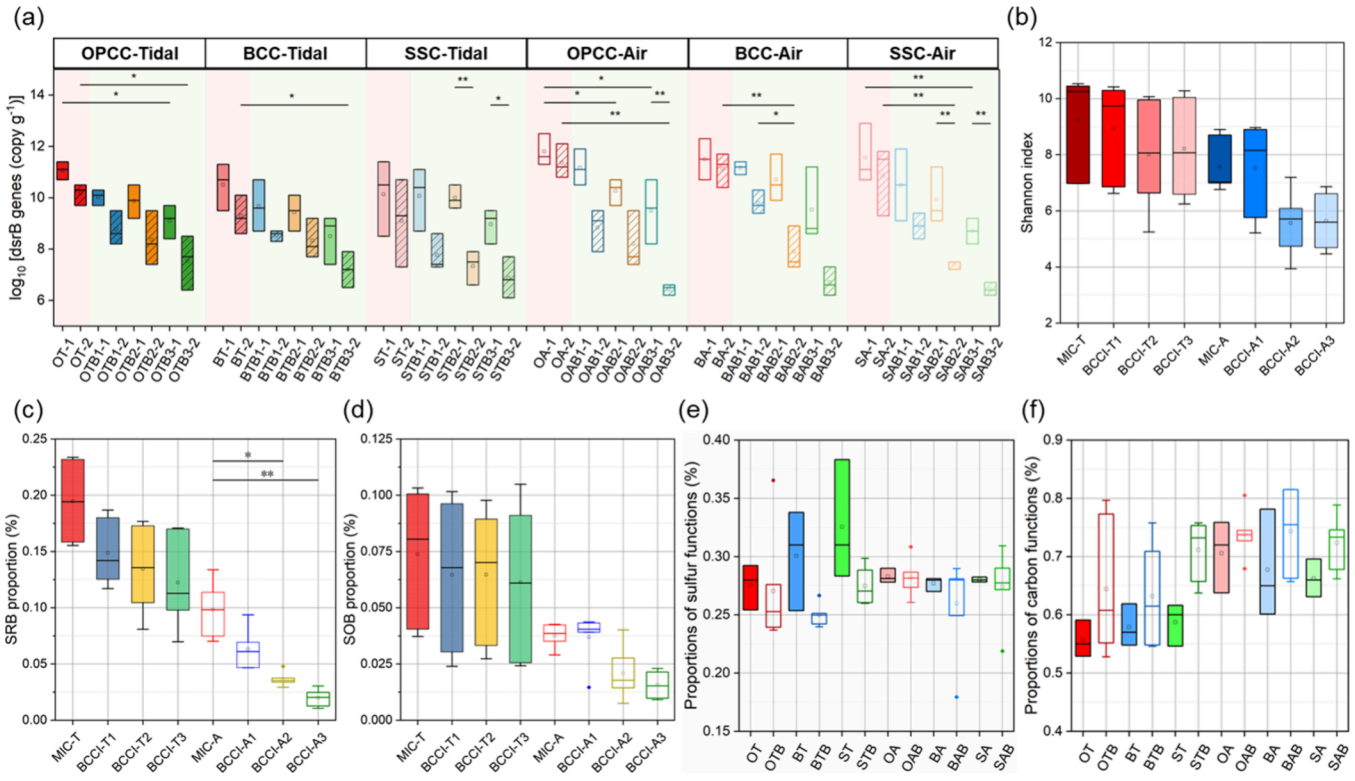

Figure 2. Panel (a) shows the qPCR analysis of evolution for concentrations of *dsrB* (copy g-1) in concrete biofilms. Panel (b) is the comparison of α diversity of biofilm communities between MIC and BCCI groups at the species level (Shannon index). Panels (c) and (d) are the comparison of SRB proportions and SOB proportions between MIC and BCCI groups, respectively. Panels (e) and (f) are the comparison of the proportions of sulfur-relevant functions and carbon-relevant functions in concrete biofilms between MIC and BCCI groups, respectively. The error bar represents the standard deviations. (** indicates a highly significant difference, $p < 0.01$; * indicates a significant difference, $p < 0.05$). Note: In Figures 2a, 2e, and 2f OT, BT, and ST denote OPCC, BCC, and SSC in the tidal zone, while OA, BA, and SA represent OPCC, BCC, and SSC in the air zone. OTB, BTB, and STB denote three types of concrete with BCCI treatment in the tidal zone. OAB, BAB, and SAB are the corresponding three types of BCCI-treated concrete in the air zone. Specifically, the first digit (1, 2, or 3) in Figure 2a corresponds to different bacterial concentrations (1×10^6 CFU/mL, 5×10^6 CFU/mL, and 1×10^7 CFU/mL), and the last digit (1 or 2) indicates the corrosion time of three or six months. Regarding Figures 2b, 2c, and 2e, MIC-T and BCCI-T include the three types of concrete specimens with different treatments in the tidal zone, while MIC-A and BCCI-A represent specimens in the air zone. Similarly, the digits 1, 2, and 3 correspond to three different bacterial concentrations.

emissions. Based on previous results, the relationship between the initial strength and the initial diffusion properties was established and GHG mitigation results corresponding to concrete production with different compressive strengths were obtained. Furthermore, concrete with a compressive strength of 55 MPa was used as the standard for underwater concrete when making conservative calculations. An assessment of GHG mitigation across 17 different countries/regions was conducted based on the obtained data on underwater concrete production in 2022 (Section S3). The details on investigating the influence of BCCI on GHG emissions are presented in Section S10.

2.6. Prediction of Global GHG Mitigation Associated with the BCCI Strategy. The global production of concrete from 2018 to 2023 was determined, and that from 2024 to 2030 was predicted based on relevant concrete market size data.[27,54] The established methods of calculation were subsequently extended to reflect and predict global GHG emissions from the production of underwater concrete from 2018 to 2030. Referring to the literature,[7] two simple scenarios ("ideal" and "realistic") were considered. Based on the discussed impact of BCCI on GHG emissions in relation to reduced diffusion properties, decreased SRB abundances, and self-healing capabilities, the global mitigation of GHG in these two scenarios was calculated after combining data from the production of underwater concrete (details of two scenarios are presented in Section S11).

3. RESULTS AND DISCUSSION

3.1. GHG Emissions in the Production of Underwater Concrete. Data on the GHG emissions from total concrete production in 17 different countries/regions showed the highest values in Mainland China, the USA, and India due to higher concrete demand (Section S12, Figure S5a). Similar trends were observed in a previous study.[55] Regarding underwater concrete, Mainland China again exhibited higher GHG emissions, followed by the USA, Indonesia, and Russia (Figure S5b). Developing countries had notably higher GHG emissions in total concrete production, up to 5.72 times more than developed countries (Figure S6). Similarly, higher GHG emissions in developing countries were observed for underwater concrete; however, the multiple dropped to 4.02 attributed to the smaller ratios of coastal cities in developing countries. These 17 different countries/regions accounted for about 83.96% of global GHG emissions in the production of underwater concrete in 2022; hence, it is crucial for these countries/regions to promptly adopt novel decarbonization strategies.

3.2. Analysis of Concrete Biofilm Communities in Field Corrosion Experiments. Compared with the MIC

https://doi.org/10.1021/acs.est.5c00261
Environ. Sci. Technol. 2025, 59, 17628−17639

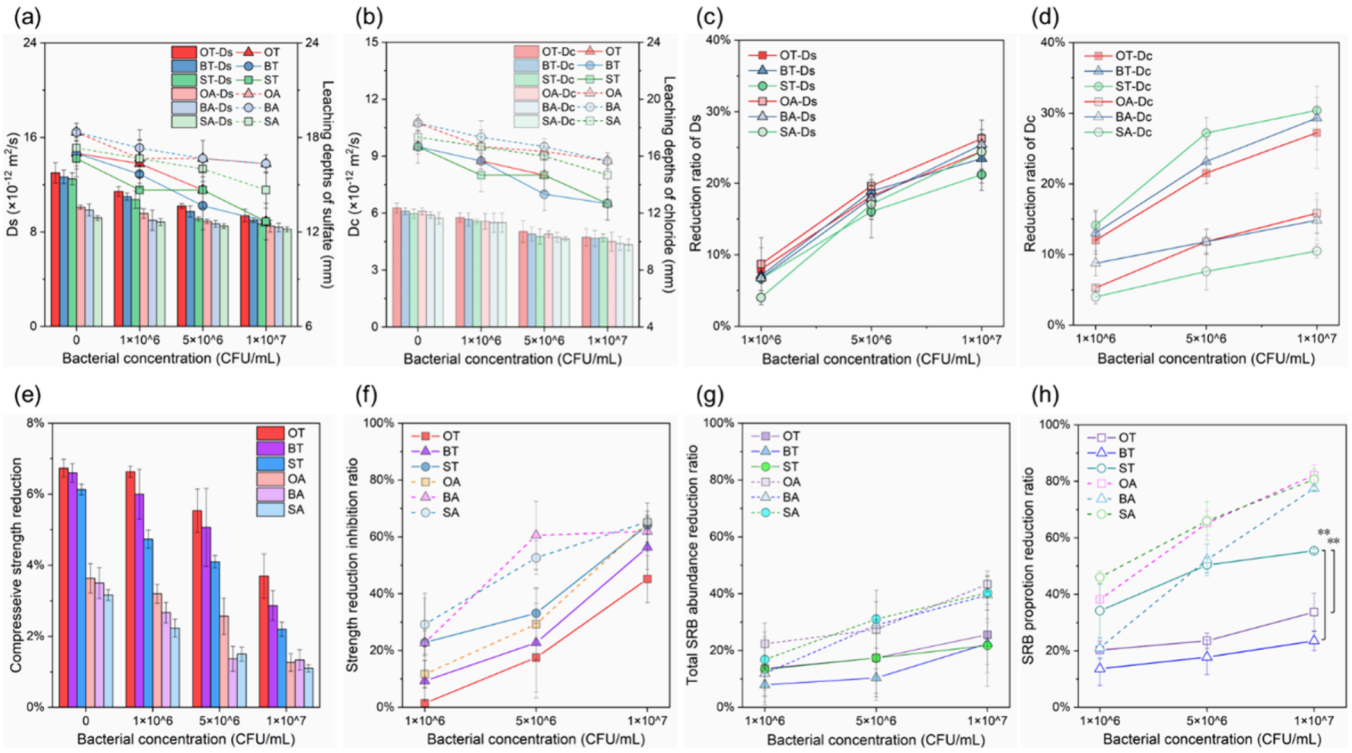

Figure 3. Panels (a) and (b) are the diffusion coefficients and leaching depths of sulfate and chloride, respectively. Panels (c) and (d) refer to the reduction ratio of diffusion coefficients of sulfate and chloride, respectively. Panel (e) and (f) are the strength reduction of concrete specimens after field corrosion and corresponding inhibition ratios resulting from BCCI. With the BCCI treatment, panels (g) and (h) show the reduction ratios of the total abundance of SRB and the SRB proportion in concrete biofilms, respectively. The error bar represents the standard deviations (** indicates a highly significant difference, $p < 0.01$; * indicates a significant difference, $p < 0.05$). Note: OT, BT, and ST refer to OPCC, BCC, and SSC in the tidal zone, while OA, BA and SA are OPCC, BCC, and SSC in the air zone.

samples, the preadded urease-producing bacteria (UPB) in the tidal groups expedited biofilm succession and decreased bacterial loads by facilitating earlier nonbacterial attachment (Section S13, Figure S7). Conversely, air samples showed higher 16S rRNA gene loads with increased concentrations of UPB, because UPB still dominated early biofilms. After three months, the MIC groups exhibited notably higher *dsrB* concentrations compared to the BCCI groups (Figure 2a), suggesting that the formation of a biomineralized film restricted SRB from accepting essential electrons for their metabolic processes,[56] despite variations in types of concrete and exposure conditions. Air groups had higher *dsrB* concentrations than the tidal groups after three months, also due to the slower development of biofilm. However, after six months, the *dsrB* concentrations of the BCCI samples with a higher UPB concentration in the air groups became lower than those in the tidal groups, probably due to stronger competition between SRB and UPB in a more stable growth environment. In the tidal groups, *dsrB* concentrations in the BCCI samples declined during corrosion because the biomineralized film effectively inhibited SRB growth.[17] The air groups showed a larger decrease in *dsrB* concentrations in the BCCI samples due to smaller nonbacterial influences. These results clearly demonstrated the effectiveness of BCCI in reducing the total abundance of SRB for different types of concrete.

BCCI reduced the diversity of the microbial community, especially with a higher UPB concentration in the air group (Figure 2b). Figure S8a shows that concrete types and exposure conditions resulted in greater influences on bacterial communities than BCCI treatment. Furthermore, the differences among the various types of concrete increased with corrosion, particularly for the SSC samples, while those between the MIC and BCCI samples diminished (Figures S8b and S8c). The genus *Sulfitobacter* from the family *Rhodobacteraceae*, which might be related to sulfur,[57] was much more abundant in the air groups (Figure S9). This might be because the tidal groups had a more mature concrete biofilm resulting from moving seawater, and the presence of other microorganisms led to a decrease in the proportions of sulfur-related bacteria. The relative abundance of SRB in the MIC samples was always greater than that in the BCCI samples (Figure S10a), with the order: MIC > BCCI1 > BCCI2 > BCCI3 (Figure 2c). Moreover, the proportions of SRB in the tidal groups were much higher than those in the air groups (Figure S10b). Biofilms result in reduced diffusion resistance, thereby eliminating distinct chemical niches, which are conducive to the proliferation of metabolically diverse microorganisms such as sulfur-related bacteria.[58] However, the biomineralized film that formed enhanced resistance performance, decreasing the proportion of SRB communities with corrosion (Figure S10c). In addition to SRB, SOB also plays a crucial role in sulfur cycling,[59] with a similarly higher proportion in the tidal group (Figure S11). The BCCI treatment also resulted in a lower relative abundance of SOB, especially with a higher concentration of UPB in the air group (Figure 2d).

Despite similar sulfur-relevant functional gene profiles in the MIC samples and BCCI samples (Figure S12a), BCCI samples had lower proportions, especially in the tidal groups (Figure 2e). However, the difference was not significant among the

https://doi.org/10.1021/acs.est.5c00261
Environ. Sci. Technol. 2025, 59, 17628−17639

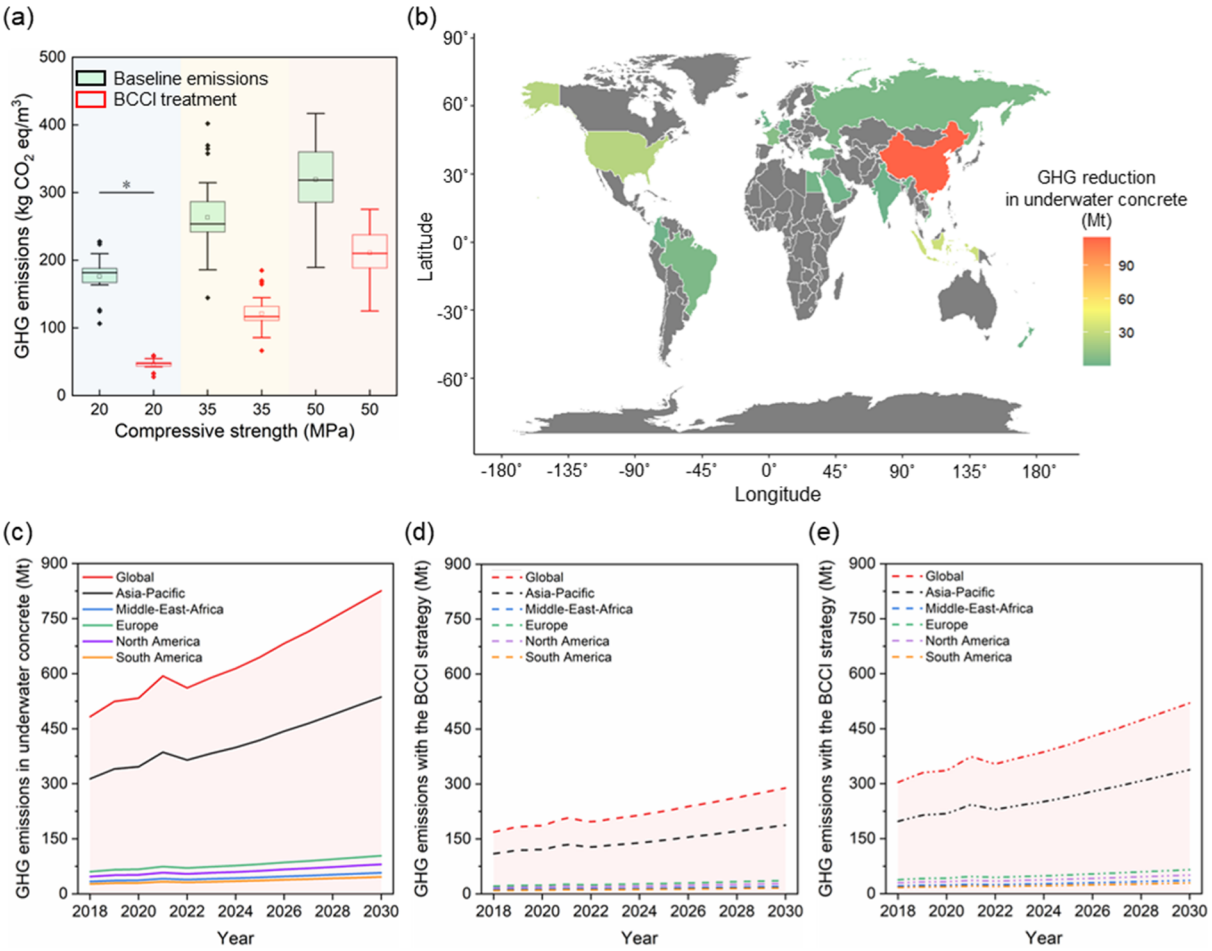

Figure 4. Panel (a) shows the influence of the BCCI strategy on GHG emissions to produce concrete with different compressive strengths. Panel (b) refers to the GHG reduction across different countries/regions based on the underwater concrete production data in 2022. Panel (c) is the global assessment of GHG emissions from underwater concrete production. Panels (d) and (e) are the prediction of global GHG mitigation associated with the proposed BCCI strategy in "ideal" and "realistic" scenarios, respectively. The error bar represents the standard deviations (** indicates a highly significant difference, $p < 0.01$; * indicates a significant difference, $p < 0.05$).

different types of concrete (Figure S12b). In addition, the BCCI treatment led to increased proportions of carbon-relevant functions (Figure 2f), with SSC in the tidal groups showing a relatively higher proportion (Figure S12c), which is probably attributable to the favorable pore solution environment for the growth of UPB. The air groups had higher proportions of carbon-relevant functions than the tidal groups due to the dominance of enriched UPB in the slowly developed biofilms. SSC differed in sulfur-relevant functions from OPCC and BCC (Figure S12d), while no substantial differences were observed in carbon-relevant functions. More lower proportions of carbon-relevant functions were observed in the MIC samples than in the BCCI samples (Figure S12e), suggesting that when the biomineralization method was utilized to inhibit sulfur-related corrosion, it also promoted carbon cycling, potentially contributing to long-term decarbonization.

3.3. Microstructural and Macroscopic Properties of Concrete in Field Corrosion Experiments. The inspection of the MIC concrete surfaces using SEM revealed a dense and uneven three-dimensional biofilm structure with embedded microbes, regardless of the type of concrete (Section S14, Figure S13). The BCCI samples exhibited relatively even biofilms due to decreased corrosive pores, where a large amount of calcite was detected via XRD (Figure S14). During the process of corrosion, the corrosive bacteria can spread across the deterioration zone, directly impairing the internal concrete structure.[60,61] The internal sulfate concentrations in the MIC samples were markedly higher than those in the BCCI samples at all depths, regardless of concrete types (Figure S15), attributed to the significant inhibitory effect on ion diffusion resulting from the biomineralized film that formed on the BCCI samples. The OPCC samples had higher internal sulfate levels, while the SSC samples exhibited the lowest concentrations. Notably, after corrosion, a convection zone was observed in the tidal groups for three types of concrete because the pores and cracks that were generated rapidly and propagated to the surface during the wetting-drying process led to a significant decline in sulfate concentrations near the surface layer. Accordingly, the MIC samples had larger diffusion coefficients of sulfate (D_S) and greater leaching depths (Figure 3a). High concentrations of sulfate can migrate from the surface to the interior layer of concrete due to alterations in the pressure gradient at the pores and cracks during the wetting-drying process.[62] Compared to the air groups, the wetting-drying process had a greater impact on the tidal groups, bringing about higher internal sulfate concentrations, which led to larger diffusion coefficients and

https://doi.org/10.1021/acs.est.5c00261
Environ. Sci. Technol. 2025, 59, 17628−17639

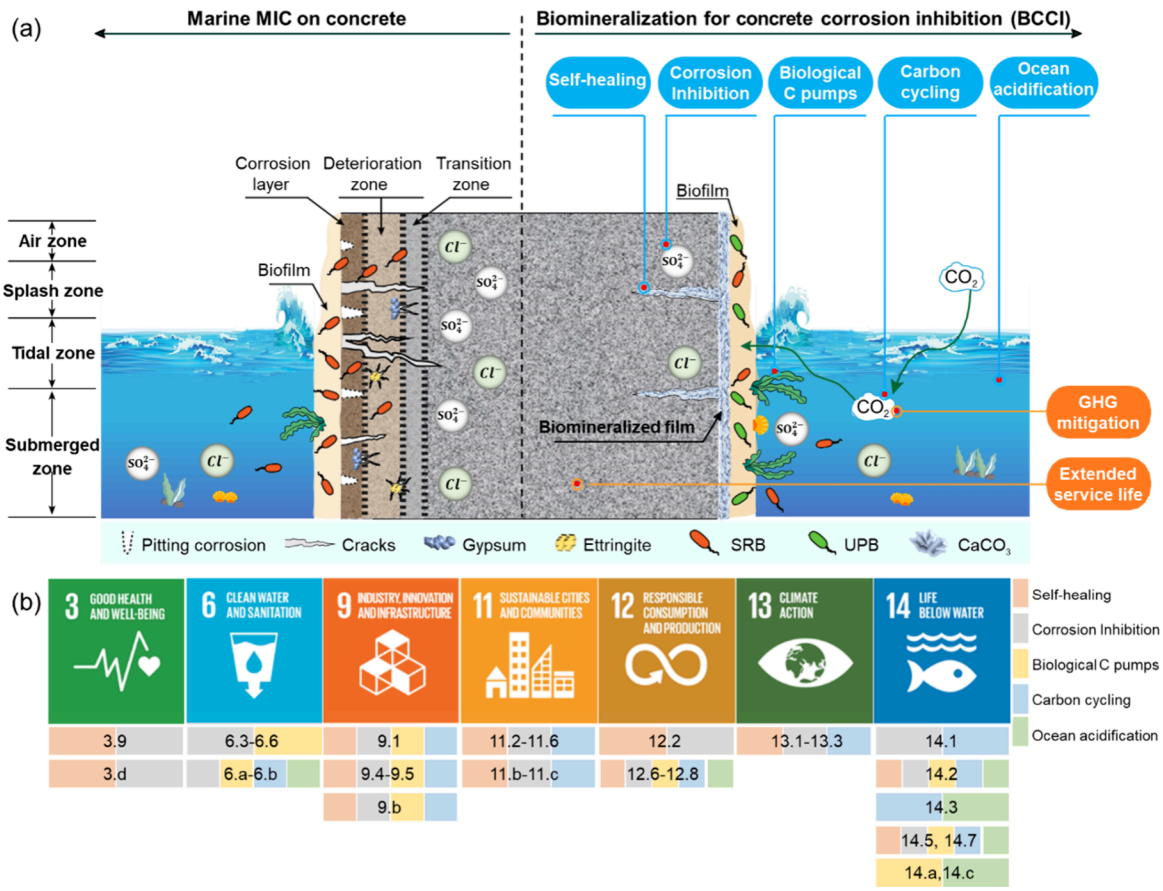

Figure 5. BCCI strategy for (a) MIC inhibition, marine concrete protection, and GHG reduction to achieve long-term decarbonization and (b) sustainable development goals (SDGs).

greater leaching depths. Regardless of concrete types or inoculations, the BCCI treatment effectively inhibited the diffusion of sulfate. Similarly, the OPCC samples had larger diffusion coefficients of chloride (D_c) and greater leaching depths than BCC and SSC (Figure 3b), and the BCCI treatment led to a significant decrease in the internal chloride levels (Figure S16). With a higher UPB concentration used for biomineralization (1×10^7 CFU/mL), the reduction ratio of D_S reached 26% for the air groups and 24% for the tidal groups (Figure 3c), coupled with reduction ratios of D_c of 15% and 28% for the air and tidal groups, respectively (Figure 3d).

Furthermore, a higher UPB concentration caused a stronger inhibitory effect due to a much higher content of $CaCO_3$ (Figure S17). The $CaCO_3$ contents varied greatly among different exposure zones; however, only marginal differences were observed among various types of concrete. Figure 3e shows the reduction in strength in all concrete specimens after six months, with OPCC exhibiting the greatest reduction, followed by BCC and SSC. Concrete in the tidal groups demonstrated a more substantial reduction in strength compared to air groups. The BCCI treatment also effectively inhibited strength reduction in different types of concrete, particularly at the highest UPB concentration, with an inhibition ratio of up to 60% for the air groups and consistently over 45% for the tidal groups (Figure 3f). This method demonstrated superior inhibition performance compared to previously reported methods for inhibiting concrete corrosion, such as using calcium aluminate concrete, self-consolidating concrete, or adding silica fume.[63,64] In addition to the role played by BCCI in inhibiting strength reduction, it also reduced the total abundance of SRB (Figure 3g) and the proportion of SRB in concrete biofilms (Figure 3h). For the tidal groups, there was a 20% reduction in the total abundance of SRB as a result of the higher UPB concentration, while reduction ratios in the proportion of SRB invariably ranged from 20% to 55%. Importantly, reduction ratios in the proportion of SRB could reach as high as 80% in the air groups because a simpler characterization during the development of biomineralized film hindered SRB growth, which similarly led to a 40% reduction in the total abundance of SRB.

3.4. Global GHG Mitigation Associated with the BCCI Strategy. According to the results of field corrosion experiments, the BCCI treatment not only inhibited the diffusion of sulfate and chloride, but also reduced the abundance of corrosive bacteria and promoted carbon cycling, all of which were beneficial for infrastructure sustainability and decarbonization. Therefore, the influence of the BCCI treatment on GHG emissions was further investigated to determine its significance and application potential. The common means to increase strength typically involves higher cement contents, which leads to greater GHG emissions,[7] resulting in a larger baseline value for the concrete with a higher compressive strength (Figure 4a). Calculations show that the BCCI treatment did indeed contribute to GHG mitigation due to increased service life. There was a significant reduction of 74% in GHG emissions for 20 MPa concrete (a difference of about 130 kg CO_2 eq/m^3). A smaller reduction of 34% in GHG emissions was observed in the 50 MPa concrete.

https://doi.org/10.1021/acs.est.5c00261
Environ. Sci. Technol. 2025, 59, 17628−17639

A possible reason for this reduction is that concrete with higher strength consistently exhibits lower initial permeability and diffusion, resulting in a smaller reduction in diffusion. The result is a comparatively smaller increase in service life and GHG mitigation. Furthermore, based on historical data on the production of underwater concrete in 2022, the calculated reduction in GHG associated with the BCCI strategy was observed to be larger in Mainland China and the USA due to their greater need for underwater concrete (Figure 4b).

Based on global data, projections of GHG emissions from total concrete production were made from 2018 to 2030 (Figure S18 in Section S15), as well as underwater concrete production (Figure 4c). The GHG mitigation potential of BCCI was estimated, considering increased lifespans and the corresponding reduced future demand for underwater concrete. The BCCI strategy offered a 2-fold benefit in this instance: (a) a substantial increase in service life, by preventing premature deterioration from chloride or sulfate ingress[17] and the accelerated effect attributed to a high abundance of corrosive bacteria; (b) the utilization of CO_2 by UPB to produce precipitates, usually allowing self-healing to further reduce GHG emissions during the operational stage.[65] Such modeling requires several assumptions on factors such as which countries/regions will have access to the BCCI strategy and the ability to use it for improved durability, which countries/regions will be susceptible to deterioration in their concrete structures and in their mechanisms for dealing with their failure, and which would consequently benefit from the use of the strategy, and the extended service life that can be anticipated. First, an "ideal" scenario was considered where all underwater concrete could be protected via the BCCI strategy. In this case, a significant reduction in global GHG emissions could be achieved, including in the Asia-Pacific area (Figure 4d). In addition, a "realistic" scenario was implemented with the BCCI strategy available in 50% of countries/regions. Significant benefits from increasing the lifespan of concrete structures were still observed, with a 37−45% reduction in GHG emissions (Figure 4e).

3.5. Potential for the Application of BCCI to Protect Underwater Concrete. The corrosion layer provides an optimal medium for microorganisms to colonize and grow in an MIC attack,[66] allowing microbial activity to spread throughout the zone of deterioration.[60] MIC resulted in significantly higher corrosion rates, greatly reducing the lifespan of concrete structures. The biomineralization treatment rapidly decreased the total/relative abundances of SRB and sulfate levels in concrete, as observed in our previous study.[17] Corrosion rates varied with concrete type as colonized surface affected the dominant taxa.[67] The effects of surface topography can prevail for long periods, not only during colonization and the early stages of the formation of biofilm.[68,69] The biofilm formation primarily relies on species traits and environmental conditions rather than on random mass immigration from the water phase.[70] Moreover, the colonized surface also affects the treatment effects of BCCI for different types of concrete. However, the field corrosion experiment in the study demonstrated BCCI's significant efficacy in inhibiting corrosion for different types of concrete, showcasing its extensive application potential. The biomineralized film that formed served as a protective layer, effectively controlling the diffusion of sulfate and chloride and isolating the concrete from seawater (Figure 5a). From a macroscopic perspective, the BCCI treatment brought higher inhibition ratios of diffusion coefficients, leaching depths, and strength reductions, irrespective of concrete type (Figures. 3**c**, **3d**, and **3g**).

There is a knowledge gap on the role of biofilms in marine concrete degradation because insufficient attention has been paid to the MIC on marine concrete. In the natural environment, the formation of concrete biofilms promotes sulfur cycling,[71] potentially due to organic carbon substrates from suspended sediments in pore solution.[72] Nevertheless, there is still insufficient evidence to substantiate whether microorganisms significantly contribute to marine concrete degradation, since biofilms sometimes play a crucial role in remediation processes[19] or act as a protective layer inhibiting corrosion.[73] Targeting the profiles of corrosive bacteria, the BCCI treatment effectively decreased the abundances of both SRB and SOB (Figures 2d and **2e**). The sulfur-relevant functions were also analyzed to gain a mechanistic understanding of the potential metabolic capability of enriched UPB in inhibiting concrete corrosion, elucidating the enigmatic relationship between SRB and the lifespan of marine concrete structures. The higher proportions of sulfur-relevant functions were seen in the MIC samples compared to those in the BCCI samples (Figure 2f). This suggests that the naturally developed marine concrete biofilm facilitated sulfur cycling and corrosion, while the biomineralized film effectively inhibited the MIC on marine concrete. Furthermore, significant reductions in the total/relative abundances of SBR for different types of concrete were also demonstrated from a microbiological perspective (Figures 3g and **3h**).

Notably, the field corrosion experiment lasted for six months, and prolonged corrosion might result in a deceleration in the rate of corrosion and reduced treatment effects. However, in this study, a conservative approach toward calculating GHG was consistently adopted. Therefore, the predictive results still effectively demonstrated the significant potential of BCCI for global GHG mitigation. In this study the treatment effects of BCCI on marine concrete were extended to underwater concrete, indicating that further studies in various MIC environments are warranted to optimize GHG calculations. In recent years, the interactions between concrete and biomineralization have been extensively investigated (*e.g.*, concrete crack repair and self-healing) with field tests conducted at globally different sites (Table S5 in Section S16). In this study, the BCCI method differed from previous commonly reported scenarios focusing on marine concrete crack repair;[74] nevertheless, previous field studies still demonstrated the superior adaptability of the biomineralization technique in different field environments. Therefore, in addition to different types of concrete, the BCCI strategy can also be applied to different countries/regions with coastal cities.

3.6. Implications for Decarbonization and Sustainable Development. The imperative to achieve net zero CO_2 emissions within the next few decades, as emphasized by numerous regulatory bodies in line with the Intergovernmental Panel on Climate Change's findings, has led to a particular focus on reducing GHG emissions from the production of cement-related materials to meet Paris Agreement and regional regulations targets.[75] However, given the challenges of eliminating GHG emissions from the production of cement-related materials,[4] it is crucial to address this issue through strategies such as demand reduction or durability enhancement.[7,76,77] For this reason, the BCCI strategy was proposed. It

https://doi.org/10.1021/acs.est.5c00261
Environ. Sci. Technol. 2025, 59, 17628−17639

involves the utilization of CO_2 for biomineralization to enhance the durability of underwater concrete structures, thereby extending the service life of marine/coastal infrastructures (Figure 5a). This process may contribute considerably toward achieving sustainable coastal cities. Moreover, concrete with BCCI also possesses a self-healing capacity, as UPB can utilize CO_2 to seal cracks during the operational stage of concrete structures,[51,52] also promoting long-term decarbonization. Comprehensively considering corrosion inhibition effects and self-healing mechanisms, the proposed BCCI strategy can reduce global GHG emissions from underwater concrete production by 37−65% (Figures 4d and **e**). More intensive use also has the potential to bring about larger GHG reductions due to localized material demand and supply and minimized need for long-distance transport.[55] Therefore, while developing countries have contributed to more GHG emissions from concrete production, they would also have larger GHG reductions associated with BCCI due to the development of coastal cities. A previous study reported that using supplementary cementitious materials benefited GHG reduction of 11−34%.[7] Compared to previously proposed strategies, the BCCI method still exhibits robust competitiveness.

Concerns may arise regarding the diminishing impact on GHG mitigation of extending the service life of underwater concrete structures due to improved building standards.[55] However, it is crucial to emphasize that MIC significantly degrades underwater concrete due to the accelerated effect of corrosive bacteria, leading to a tendency to overestimate their lifespans. Therefore, greater attention should be given to recognizing the decarbonization potential of extending the lifespan of underwater concrete. Furthermore, the biofilm anticorrosion durability remains a significant concern due to the inherent susceptibility to dispersion and dissolution.[73] The biomineralization treatment process also caused a small carbon footprint and consumed energy. However, subsequent colonization of nonbacteria on the top of the biomineralized film as the concrete biofilms matured, enhanced the stability of the biomineralized film, rendering it resistant to environmental disturbances and guaranteeing the durability of the treatment. This suggests that a single biomineralization treatment sufficed, resulting in significantly smaller GHG emissions compared to the overall reduction in GHG. In addition, relevant data across different exposure zones were averaged to simplify the calculations. However, the tidal zone and air zone generally exhibited the most rapid and lowest corrosion rates,[78,79] respectively, indicating that an average value would provide more instructive insights. Therefore, GHG calculation results are valuable for reference.

Several previous CO_2 mineralization techniques in concrete exhibited decarbonization potential with 0.01−0.49 CO_2 eq/kg. These techniques are often limited during the material preparation stage.[80] The proposed BCCI method can be regarded as a novel CO_2 mineralization technique related to concrete materials with a superior decarbonization capability, which can be applied in both the material preparation stage and the operational phase. In addition, this GHG calculation model solely focused on diffusion properties and corrosive bacteria, without considering the further influence of biomineralized bacteria. The biomineralized film that formed not only inhibited sulfur-related corrosion, but also increased the proportions of carbon-relevant functions (Figure 2g), suggesting that this innovative technique holds greater potential for promoting carbon cycling (Figure 5a). As the ocean is the largest active carbon reservoir,[81] the enhanced carbon cycling in the marine concrete biofilms may further contribute to carbon neutrality and negative carbon emissions, thereby mitigating the issue of ocean acidification and stabilizing marine ecosystems. Moreover, the BCCI treatment expedited the development of concrete biofilms through preadded UPB, facilitating the rapid attachment and growth of nonbacteria (*e.g.,* microalgae or diatoms) (Figure S9). The attached microalgae or diatoms can serve as effective biological carbon pumps for CO_2 capture and organic matter production.[81,82] This dual potential of the BCCI treatment, namely mitigating ocean acidification and promoting the formation of biological carbon pumps, also contributes to long-term decarbonization and environmental preservation. The capacities of BCCI (corrosion inhibition and self-healing) offer significant benefits for enhancing the stability and protection of buildings in coastal cities. The future advantages of BCCI pertaining to carbon cycling, ocean acidification, and biological carbon pumps hold great potential for the stabilization of marine ecosystems, thereby fostering the survival of shellfish and corals. These five aspects of BCCI were related to several SDGs[83] (Figure 5b) (detailed contents are presented in Section S17). Consequently, the proposed BCCI strategy could kill two birds with one stone, achieving both global decarbonization and multiple SDGs.

■ ASSOCIATED CONTENT

Supporting Information

The Supporting Information is available free of charge at https://pubs.acs.org/doi/10.1021/acs.est.5c00261.

> Methodology and pipelines used in this study, the analysis of baseline GHG emissions, details of the arrangements relating to the field corrosion experiment, the process of analyzing microbial communities and the functional annotations of biofilms, the measurements of the microstructural and mechanical properties of concrete, the relationships established in the GHG calculations and the potential influence of BCCI, the prediction of global GHG mitigation from the BCCI strategy, the analysis of the genotypic data of biofilms including communities and functional microorganisms and genes, the microstructural characteristics of concrete biofilms, the profiles of sulfate and chloride in concrete, the potential mitigation effects of the proposed BCCI strategy, and the global field application trials of biomineralization in concrete structures, coupled with the relationship between BCCI and SDGs (PDF)

■ AUTHOR INFORMATION

Corresponding Author

Xiangdong Li − *Department of Civil and Environmental Engineering and Research Institute for Sustainable Urban Development, The Hong Kong Polytechnic University, Hong Kong SAR, China;* orcid.org/0000-0002-4044-2888; Phone: (852) 2766-6041; Email: cexdli@polyu.edu.hk; Fax: (852) 2334-6389

Authors

Xiaohao Sun − *Department of Civil and Environmental Engineering, The Hong Kong Polytechnic University, Hong Kong SAR, China;* orcid.org/0000-0001-6234-3023

Yong Wang − *Department of Civil and Environmental Engineering, The Hong Kong Polytechnic University, Hong Kong SAR, China*
Jiadong Ren − *Department of Civil and Environmental Engineering, The Hong Kong Polytechnic University, Hong Kong SAR, China;* orcid.org/0009-0001-3985-9336
Onyx W.H. Wai − *Department of Civil and Environmental Engineering and Research Institute for Sustainable Urban Development, The Hong Kong Polytechnic University, Hong Kong SAR, China*

Complete contact information is available at: https://pubs.acs.org/10.1021/acs.est.5c00261

Author Contributions

X-H.S., O.W−H.W., and X-D.L. designed the study. X-H.S. performed the calculations and experiments. Y.W. and J-D.R. collected data. X-H.S., Y.W., and J-D.R. analyzed the data. X-H.S. and X-D.L. wrote the paper with input from all of the authors. All of the authors read and approved the final manuscript.

Notes

The authors declare no competing financial interest.

■ ACKNOWLEDGMENTS

This study was funded by the Hong Kong Research Grants Council (project no. T22-502/18-R), the National Natural Science Foundation of China (22193063), the Strategic Priority Research Program of the Chinese Academy of Sciences (XDB40020102), the Hong Kong Green Technology Fund (GTF202310277), and the Research Institute for Sustainable Urban Development (RISUD) at The Hong Kong Polytechnic University. The authors thank the Concrete Materials Laboratory in the Department of Civil and Environmental Engineering for providing the SEM equipment and the University Research Facility in Big Data Analytics (UBDA) at The Hong Kong Polytechnic University for providing a data analysis platform.

■ REFERENCES

(1) Monteiro, P. J.; Miller, S. A.; Horvath, A. Towards sustainable concrete. *Nat. Mater.* **2017**, *16* (7), 698−699.
(2) Maddalena, R.; Roberts, J. J.; Hamilton, A. Can Portland cement be replaced by low-carbon alternative materials? A study on the thermal properties and carbon emissions of innovative cements. *J. Cleaner Prod.* **2018**, *186*, 933−942.
(3) Summerbell, D. L.; Barlow, C. Y.; Cullen, J. M. Potential reduction of carbon emissions by performance improvement: A cement industry case study. *J. Cleaner Prod.* **2016**, *135*, 1327−1339.
(4) Davis, S. J.; Lewis, N. S.; Shaner, M.; Aggarwal, S.; Arent, D.; Azevedo, I. L.; Benson, S. M.; Bradley, T.; Brouwer, J.; Chiang, Y. M.; et al. Net-zero emissions energy systems. *Science* **2018**, *360* (6396), No. eaas9793.
(5) UNPD *The World's Cities in 2018-Data Booklet*; United Nations: **2018**, 1-34.
(6) Miller, S. A. The role of cement service-life on the efficient use of resources. *Environ. Res. Lett.* **2020**, *15* (2), No. 024004.
(7) Olsson, J. A.; Miller, S. A.; Alexander, M. G. Near-term pathways for decarbonizing global concrete production. *Nat. Commun.* **2023**, *14* (1), 4574.
(8) Peng, L.; Zhao, Y.; Ban, J.; Wang, Y.; Shen, P.; Lu, J. X.; Poon, C. S. Enhancing the corrosion resistance of recycled aggregate concrete by incorporating waste glass powder. *Cem. Concr. Compos.* **2023**, *137*, No. 104909.
(9) Li, Y.; Xu, D.; Chen, C.; Li, X.; Jia, R.; Zhang, D.; Sand, W.; Wang, F.; Gu, T. Anaerobic microbiologically influenced corrosion mechanisms interpreted using bioenergetics and bioelectrochemistry: a review. *J. Mater. Sci. Technol.* **2018**, *34* (10), 1713−1718.
(10) Li, X.; Lin, X.; Lin, K.; Ji, T. Study on the degradation mechanism of sulphoaluminate cement sea sand concrete eroded by biological sulfuric acid. *Constr. Build. Mater.* **2017**, *157*, 331−336.
(11) Wu, M.; Wang, T.; Wu, K.; Kan, L. Microbiologically induced corrosion of concrete in sewer structures: A review of the mechanisms and phenomena. *Constr. Build. Mater.* **2020**, *239*, No. 117813.
(12) Xu, D.; Jia, R.; Li, Y.; Gu, T. Advances in the treatment of problematic industrial biofilms. *World J. Microbiol. Biotechnol.* **2017**, *33*, 97.
(13) Zhong, H.; Shi, Z.; Jiang, G.; Yuan, Z. Decreasing microbially influenced metal corrosion using free nitrous acid in a simulated water injection system. *Water Res.* **2020**, *172*, No. 115470.
(14) Ali, H. A.; Xuan, D.; Lu, J. X.; Poon, C. S. Enhancing the resistance to microbial induced corrosion of alkali-activated glass powder/GGBS mortars by calcium aluminate cement. *Constr. Build. Mater.* **2022**, *341*, No. 127912.
(15) Han, S.; Zhong, J.; Yu, Q.; Yan, L.; Ou, J. Sulfate resistance of eco-friendly and sulfate-resistant concrete using seawater sea-sand and high-ferrite Portland cement. *Constr. Build. Mater.* **2021**, *305*, No. 124753.
(16) Xie, Y.; Lin, X.; Ji, T.; Liang, Y.; Pan, W. Comparison of corrosion resistance mechanism between ordinary Portland concrete and alkali-activated concrete subjected to biogenic sulfuric acid attack. *Constr. Build. Mater.* **2019**, *228*, No. 117071.
(17) Sun, X.; Wai, O. W. H.; Xie, J.; Li, X. D. Biomineralization to prevent microbially induced corrosion on concrete for sustainable marine infrastructure. *Environ. Sci. Technol.* **2024**, *58* (1), 522−533.
(18) Bao, J.; Wei, J.; Zhang, P.; Zhuang, Z.; Zhao, T. Experimental and theoretical investigation of chloride ingress into concrete exposed to real marine environment. *Cem. Concr. Compos.* **2022**, *130*, No. 104511.
(19) Sun, X.; Miao, L.; Wu, L.; Wang, H. Theoretical quantification for cracks repair based on microbially induced carbonate precipitation (MICP) method. *Cem. Concr. Compos.* **2021**, *118*, No. 103950.
(20) Zeng, J.; Bi, Z.; Xu, J.; Chen, Q.; Zhu, H. Biomineralized coating inhibiting corrosion of reinforcement in cracked concrete: A study in simulated aggressive environments. *J. Build. Eng.* **2025**, *101*, No. 111889.
(21) O'Connell, M.; McNally, C.; Richardson, M. G. Performance of concrete incorporating GGBS in aggressive wastewater environments. *Constr. Build. Mater.* **2012**, *27* (1), 368−374.
(22) Hughes, P.; Fairhurst, D.; Sherrington, I.; Renevier, N.; Morton, L. H. G.; Robery, P.; Cunningham, L. Microscopic study into biodeterioration of marine concrete. *Int. Biodeterior. Biodegrad.* **2013**, *79*, 14−19.
(23) Cheng, L.; House, M. W.; Weiss, W. J.; Banks, M. K. Monitoring sulfide-oxidizing biofilm activity on cement surfaces using non-invasive self-referencing microsensors. *Water Res.* **2016**, *89*, 321−329.
(24) Song, Y.; Chetty, K.; Garbe, U.; Wei, J.; Bu, H.; O'Moore, L.; Li, X.; Yuan, Z.; McCarthy, T.; Jiang, G. A novel granular sludge-based and highly corrosion-resistant bio-concrete in sewers. *Sci. Total Environ.* **2021**, *791*, No. 148270.
(25) Churkina, G.; Organschi, A.; Reyer, C. P. O.; Ruff, A.; Vinke, K.; Liu, Z.; Reck, B. K.; Graedel, T. E.; Schellnhuber, H. J. Buildings as a global carbon sink. *Nat. Sustain.* **2020**, *3* (4), 269−276.
(26) Kim, A.; Cunningham, P. R.; Kamau-Devers, K.; Miller, S. A. OpenConcrete: a tool for estimating the environmental impacts from concrete production. *Environ. Res.: Infrastruct. Sustainability* **2022**, *2* (4), No. 041001.
(27) Markets and Markets *Underwater Concrete Market Research Report*. United States. **2023**. www.marketsandmarkets.com/pdfdownloadNew.asp?id=155024605.pdf.
(28) Chen, B.; Liang, X.; Huang, X.; Zhang, T.; Li, X. D. Differentiating anthropogenic impacts on ARGs in the Pearl River

Estuary by using suitable gene indicators. *Water Res.* **2013**, *47* (8), 2811−2820.
(29) Cai, W.; Li, Y.; Niu, L.; Zhang, W.; Wang, C.; Wang, P.; Meng, F. New insights into the spatial variability of biofilm communities and potentially negative bacterial groups in hydraulic concrete structures. *Water Res.* **2017**, *123*, 495−504.
(30) Rajala, P.; Cheng, D. Q.; Rice, S. A.; Lauro, F. M. Sulfate-dependant microbially induced corrosion of mild steel in the deep sea: a 10-year microbiome study. *Microbiome* **2022**, *10* (1), 4.
(31) Foox, J.; Tighe, S. W.; Nicolet, C. M.; Zook, J. M.; Byrska-Bishop, M.; Clarke, W. E.; Khayat, M. M.; Mahmoud, M.; Laaguiby, P. K.; Herbert, Z. T.; Warner, D.; Grills, G. S.; Jen, J.; Levy, S.; Xiang, J.; Alonso, A.; Zhao, X.; Zhang, W.; Teng, F.; Zhao, Y.; Lu, H.; Schroth, G. P.; Narzisi, G.; Farmerie, W.; Sedlazeck, F. J.; Baldwin, D. A.; Mason, C. E. Performance assessment of DNA sequencing platforms in the ABRF Next-Generation Sequencing Study. *Nat. Biotechnol.* **2021**, *39* (9), 1129−1140.
(32) Chen, S.; Zhou, Y.; Chen, Y.; Gu, J. fastp: an ultra-fast all-in-one FASTQ preprocessor. *Bioinformatics* **2018**, *34* (17), i884−i890.
(33) Wood, D. E.; Lu, J.; Langmead, B. Improved metagenomic analysis with Kraken 2. *Genome Biol.* **2019**, *20*, 257.
(34) Lu, J.; Breitwieser, F. P.; Thielen, P.; Salzberg, S. L. Bracken: estimating species abundance in metagenomics data. *PeerJ. Comput. Sci.* **2017**, *3*, No. e104.
(35) Lozupone, C.; Knight, R. UniFrac: a new phylogenetic method for comparing microbial communities. *Appl. Environ. Microbiol.* **2005**, *71* (12), 8228−8235.
(36) Uritskiy, G. V.; DiRuggiero, J.; Taylor, J. MetaWRAP—a flexible pipeline for genome-resolved metagenomic data analysis. *Microbiome* **2018**, *6* (1), 158.
(37) Kim, D.; Song, L.; Breitwieser, F. P.; Salzberg, S. L. Centrifuge: rapid and sensitive classification of metagenomic sequences. *Genome Res.* **2016**, *26* (12), 1721−1729.
(38) Hyatt, D.; Chen, G. L.; LoCascio, P. F.; Land, M. L.; Larimer, F. W.; Hauser, L. J. Prodigal: prokaryotic gene recognition and translation initiation site identification. *BMC Bioinf.* **2010**, *11*, 119.
(39) Cantalapiedra, C. P.; Hernández-Plaza, A.; Letunic, I.; Bork, P.; Huerta-Cepas, J. eggNOG-mapper v2: functional annotation, orthology assignments, and domain prediction at the metagenomic scale. *Mol. Biol. Evol.* **2021**, *38* (12), 5825−5829.
(40) Kanehisa, M.; Goto, S.; Sato, Y.; Furumichi, M.; Tanabe, M. KEGG for integration and interpretation of large-scale molecular data sets. *Nucleic Acids Res.* **2012**, *40* (D1), D109−D114.
(41) Bray, J. R.; Curtis, J. T. An ordination of the upland forest communities of southern Wisconsin. *Ecol. Monogr.* **1957**, *27* (4), 326−349.
(42) Wang, H.; Yang, Q.; Li, D.; Wu, J.; Yang, S.; Deng, Y.; Luo, C.; Jia, W.; Zhong, Y.; Peng, P. Stable Isotopic and Metagenomic Analyses Reveal Microbial-Mediated Effects of Microplastics on Sulfur Cycling in Coastal Sediments. *Environ. Sci. Technol.* **2023**, *57* (2), 1167−1176.
(43) Cai, Y.; Xuan, D.; Hou, P.; Shi, J.; Poon, C. S. Effect of seawater as mixing water on the hydration behaviour of tricalcium aluminate. *Cem. Concr. Res.* **2021**, *149*, No. 106565.
(44) Ismail, I.; Bernal, S. A.; Provis, J. L.; Hamdan, S.; van Deventer, J. S. Microstructural changes in alkali activated fly ash/slag geopolymers with sulfate exposure. *Mater. Struct.* **2013**, *46*, 361−373.
(45) Zou, D.; Qin, S.; Liu, T.; Jivkov, A. Experimental and numerical study of the effects of solution concentration and temperature on concrete under external sulfate attack. *Cem. Concr. Res.* **2021**, *139*, No. 106284.
(46) Sun, X.; Miao, L.; Tong, T.; Wang, C. Improvement of microbial-induced calcium carbonate precipitation technology for sand solidification. *J. Mater. Civ. Eng.* **2018**, *30* (11), No. 04018301.
(47) Maali, M.; Showkati, H.; Fatemi, S. M. Investigation of the buckling behavior of conical shells under weld-induced imperfections. *Thin-Walled Struct.* **2012**, *57*, 13−24.
(48) Sun, Y. M.; Chang, T. P.; Liang, M. T. Service life prediction for concrete structures by time-depth dependent chloride diffusion coefficient. *J. Mater. Civ. Eng.* **2010**, *22* (11), 1187−1190.
(49) Lee, H.; Cho, M.-S.; Lee, J.-S.; Kim, D.-G. Prediction model of life span degradation under sulfate attack regarding diffusion rate by amount of sulfate ions in seawater. *Int. J. Mater. Mech. Manuf* **2013**, *1* (3), 251−255.
(50) Jin, L.; Qiao, L.; Liu, P.; Wang, Z.; Wu, T.; Wu, Q.; Zhou, P. Reliability-based life prediction method for concrete sewage pipelines under microbial attack. *Mater. Today Commun.* **2024**, *39*, No. 108621.
(51) Justo-Reinoso, I.; Arena, N.; Reeksting, B. J.; Gebhard, S.; Paine, K. Bacteria-based self-healing concrete− A life cycle assessment perspective. *Developments in the Built Environment* **2023**, *16*, No. 100244.
(52) Wang, J.; Snoeck, D.; Van Vlierberghe, S.; Verstraete, W.; De Belie, N. Application of hydrogel encapsulated carbonate precipitating bacteria for approaching a realistic self-healing in concrete. *Constr. Build. Mater.* **2014**, *68*, 110−119.
(53) Basilisk, self healing concrete *Basilisk Info sheet No. 7*. The Netherlands, Delft, **2020**.
(54) Mordor Intelligence *Ready Mix Concrete Market Size & Share Analysis - Growth trends & Forecasts up to 2030*. India, **2024**. www.mordorintelligence.com/industry-reports/ready-mix-concrete-market.pdf.
(55) Zhong, X.; Hu, M.; Deetman, S.; Steubing, B.; Lin, H. X.; Hernandez, G. A.; Harpprecht, C.; Zhang, C.; Tukker, A.; Behrens, P. Global greenhouse gas emissions from residential and commercial building materials and mitigation strategies to 2060. *Nat. Commun.* **2021**, *12* (1), 6126.
(56) Gu, T.; Jia, R.; Unsal, T.; Xu, D. Toward a better understanding of microbiologically influenced corrosion caused by sulfate reducing bacteria. *J. Mater. Sci. Technol.* **2019**, *35* (4), 631−636.
(57) Barak-Gavish, N.; Frada, M. J.; Ku, C.; Lee, P. A.; DiTullio, G. R.; Malitsky, S.; Aharoni, A.; Green, S. J.; Rotkopf, R.; Kartvelishvily, E.; Sheyn, U.; Schatz, D.; Vardi, A. Bacterial virulence against an oceanic bloom-forming phytoplankter is mediated by algal DMSP. *Sci. Adv.* **2018**, *4* (10), No. eaau5716.
(58) Stewart, P. S. Diffusion in biofilms. *J. Bacteriol.* **2003**, *185* (5), 1485−1491.
(59) Erbektas, A. R.; Isgor, O. B.; Weiss, W. J. An accelerated testing protocol for assessing microbially induced concrete deterioration during the bacterial attachment phase. *Cem. Concr. Compos.* **2019**, *104*, No. 103339.
(60) Grengg, C.; Mittermayr, F.; Koraimann, G.; Konrad, F.; Szabó, M.; Demeny, A.; Dietzel, M. The decisive role of acidophilic bacteria in concrete sewer networks: A new model for fast progressing microbial concrete corrosion. *Cem. Concr. Res.* **2017**, *101*, 93−101.
(61) Ouyang, X.; Koleva, D. A.; Ye, G.; van Breugel, K. Understanding the adhesion mechanisms between CSH and fillers. *Cem. Concr. Res.* **2017**, *100*, 275−283.
(62) Cheng, S.; Wu, Z.; Wu, Q.; Chen, X.; Shui, Z.; Lu, J.-X. Degradation characteristics of Portland cement mortar incorporating supplementary cementitious materials under multi-ions attacks and drying-wetting cycles. *J. Cleaner Prod.* **2022**, *363*, No. 132378.
(63) Ehrich, S.; Helard, L.; Letourneux, R.; Willocq, J.; Bock, E. Biogenic and Chemical Sulfuric Acid Corrosion of Mortars. *J. Mater. Civ. Eng.* **1999**, *11* (4), 340−344.
(64) Alaghebandian, N.; Mirvalad, S.; Javid, A. A. S. Durability of self-consolidating concrete and mortar mixtures containing ternary and quaternary cement blends exposed to simulated marine environment. *Constr. Build. Mater.* **2020**, *259*, No. 119767.
(65) Van Belleghem, B.; Van den Heede, P.; Van Tittelboom, K.; De Belie, N. Quantification of the service life extension and environmental benefit of chloride exposed self-healing concrete. *Materials* **2017**, *10* (1), 5.
(66) Monteny, J.; Vincke, E.; Beeldens, A.; De Belie, N.; Taerwe, L.; Van Gemert, D.; Verstraete, W. Chemical, microbiological, and in situ test methods for biogenic sulfuric acid corrosion of concrete. *Cem. Concr. Res.* **2000**, *30* (4), 623−634.

https://doi.org/10.1021/acs.est.5c00261
Environ. Sci. Technol. 2025, 59, 17628−17639

(67) Antunes, J.; Leão, P.; Vasconcelos, V. Marine biofilms: diversity of communities and of chemical cues. *Environ. Microbiol. Rep.* **2019**, *11* (3), 287−305.
(68) Jones, A. A.; Bennett, P. C. Mineral ecology: surface specific colonization and geochemical drivers of biofilm accumulation, composition, and phylogeny. *Front. Microbiol.* **2017**, *8*, 491.
(69) Zhang, W. P.; Wang, Y.; Tian, R. M.; Bougouffa, S.; Yang, B.; Cao, H. L.; Zhang, G.; Wong, Y. H.; Xu, W.; Batang, Z.; Al-Suwailem, A.; Zhang, X. X.; Qian, P. Y. Species sorting during biofilm assembly by artificial substrates deployed in a cold seep system. *Sci. Rep.* **2014**, *4* (1), 6647.
(70) Karačić, S.; Modin, O.; Hagelia, P.; Persson, F.; Wilén, B.-M. The effect of time and surface type on the composition of biofilm communities on concrete exposed to seawater. *Int. Biodeterior. Biodegrad.* **2022**, *173*, No. 105458.
(71) Li, Y.; Wan, M.; Du, J.; Lin, L.; Cai, W.; Wang, L. Microbial enhanced corrosion of hydraulic concrete structures under hydrodynamic conditions: Microbial community composition and functional prediction. *Constr. Build. Mater.* **2020**, *248*, No. 118609.
(72) Seeley, M. E.; Song, B.; Passie, R.; Hale, R. C. Microplastics affect sedimentary microbial communities and nitrogen cycling. *Nat. Commun.* **2020**, *11*, 2372.
(73) Guo, N.; Wang, Y.; Hui, X.; Zhao, Q.; Zeng, Z.; Pan, S.; Guo, Z.; Yin, Y.; Liu, T. Marine bacteria inhibit corrosion of steel via synergistic biomineralization. *J. Mater. Sci. Technol.* **2021**, *66*, 82−90.
(74) Fan, Q.; Fan, L.; Quach, W.-M.; Zhang, R.; Duan, J.; Sand, W. Application of microbial mineralization technology for marine concrete crack repair: A review. *J. Build. Eng.* **2023**, *69*, No. 106299.
(75) Obrist, M. D.; Kannan, R.; Schmidt, T. J.; Kober, T. Decarbonization pathways of the Swiss cement industry towards net zero emissions. *J. Cleaner Prod.* **2021**, *288*, No. 125413.
(76) Miller, S. A.; Habert, G.; Myers, R. J.; Harvey, J. T. Achieving net zero greenhouse gas emissions in the cement industry via value chain mitigation strategies. *One Earth* **2021**, *4* (10), 1398−1411.
(77) Hertwich, E. G.; Ali, S.; Ciacci, L.; Fishman, T.; Heeren, N.; Masanet, E.; Asghari, F. N.; Olivetti, E.; Pauliuk, S.; Tu, Q.; Wolfram, P. Material efficiency strategies to reducing greenhouse gas emissions associated with buildings, vehicles, and electronics—a review. *Environ. Res. Lett.* **2019**, *14* (4), No. 043004.
(78) Liu, Q.; Sun, L.; Zhu, X.; Xu, L.; Zhao, G. Chloride transport in the reinforced concrete column under the marine environment: Distinguish the atmospheric, tidal-splash and submerged zones. *Structures* **2022**, *39*, 365−377.
(79) Abd El Fattah, A.; Al-Duais, I.; Riding, K.; Thomas, M. Field evaluation of corrosion mitigation on reinforced concrete in marine exposure conditions. *Constr. Build. Mater.* **2018**, *165*, 663−674.
(80) Driver, J. G.; Bernard, E.; Patrizio, P.; Fennell, P. S.; Scrivener, K.; Myers, R. J. Global decarbonization potential of CO2 mineralization in concrete materials. *Proc. Natl. Acad. Sci. U. S. A.* **2024**, *121* (29), No. e2313475121.
(81) Jiao, N.; Zhu, C.; Liu, J.; Luo, T.; Bai, M.; Yu, Z.; Chen, Q.; Rinkevich, B.; Weinbauer, M.; Thomas, H.; Fernández-Méndez, M.; López-Abbate, C.; Signori, C. N.; Nagappa, R.; Koblížek, M.; Kaartokallio, H.; Hyun, J. H.; Jiao, F.; Chen, F.; Cai, W. J. A roadmap for Ocean Negative Carbon Emission eco-engineering in sea-farming fields. *Innovation Geosci.* **2023**, *1* (2), No. 100029.
(82) Wang, W. L.; Fu, W.; Le Moigne, F. A. C.; Letscher, R. T.; Liu, Y.; Tang, J. M.; Primeau, F. W. Biological carbon pump estimate based on multidecadal hydrographic data. *Nature* **2023**, *624* (7992), 579−585.
(83) Zhang, Y.; Xu, W.; Zhu, X.; Maboudian, R.; Ok, Y. S.; Tsang, D. C. Scaling biochar solutions for urban carbon dioxide removal. *One Earth* **2024**, *7* (9), 1481−1486.

https://doi.org/10.1021/acs.est.5c00261
Environ. Sci. Technol. 2025, 59, 17628−17639